Calibration of neutron detectors at ASDEX Upgrade, measurement and model

Monika Koleva[a], Giovanni Tardini[a], Hartmut Zohm[a], Simppa Äkäslompolo[b], Jaakko Leppänen[c], and the ASDEX Upgrade Team[a]

[a] *Max-Planck-Institute for Plasma Physics, 85748 Garching, Germany*
[b] *Aalto University, Otakaari 1 B, 02150 Espoo, Finland*
[c] *VTT Technical Research Centre of Finland, Kivimiehentie, 02150, Espoo, Finland*

Abstract

The neutron production in ASDEX Upgrade (AUG) neutral beam injection (NBI) heated discharges is dominated by beam-target fusion reactions. Hence, the neutron rate (NR) and energy distributions are footprints of the fast ion distribution. This motivates to establish a reliable neutron rate calibration. Comparisons at AUG between the experimental NR and the one predicted by the TRANSP code show systematic variations from campaign to campaign. Potential reason for this is the delicate absolute calibration of the neutron detectors. Therefore, a different calibration technique was performed, enabling longer acquisition time, uniform geometry, better statistics and thus less uncertainty. A toy train carrying a radioactive source (^{238}Pu/B) over two radial positions on the equatorial plane shows a periodical NR on the epithermal ^{3}He neutron detector. The calibration results are compared to a neutron transport simulation using the Monte Carlo (MC) code Serpent. Preliminary comparisons for one source position on the outer railway track show a discrepancy factor of about 130 in the position of least material inside the simulation, in the direct line of sight to the detector. For a better understanding of these results, two additional measurements were performed. The results were again compared to a detailed Serpent simulation. This paper describes the calibration set-up for the neutron measurements in AUG, provides a brief simulation background on reaction rate estimations and a survey on the comparison between the measured and calculated neutron rates.

Keywords: Calibration, Neutron detector, Monte Carlo transport code, Serpent code

1. Introduction

Research fusion facilities mostly operate with deuterium (D-D) fuel which produces neutrons of 2.45 MeV energy. In neutral beam injection (NBI) heated discharges, the fast ions reacting with the bulk plasma (beam-target reactions) dominate the neutron rate (NR). Thus, the NR is an imprint of the fast particles, which can drive instabilities and damage the plasma facing components (PFC) [1, 2]. Accurate neutron measurements and a reasonable agreement between experiment and theoretical calculations are therefore essential to understanding the fast ion dynamics.

Over the course of NR investigations at ASDEX Upgrade (AUG), comparisons between the experimental and the NR predicted by the TRANSP code [3] show systematic deviations between calibration campaigns, which may point to potential calibration errors in the neutron detectors. The calibration has been found accurate to about 40% [2]. In comparison, the statistical uncertainty in 1 millisecond binning, which is roughly 4%, and could be minimized with the choice of binning, is negligible. The usual way to calibrate involved the probing of a few discrete source positions inside the machine which did not have high statistics and were hard to reproduce precisely over the years. This has prompted us to carry out an ab initio absolute calibration with more reproducible geometry, better count statistics and the utilization of a comprehensive Monte Carlo simulation [4, 5, 6] for neutron transport and detection using the Serpent code [7].

2. Calibration set-up for neutron measurements at AUG

Complex geometries like tokamaks and stellarators are organized in sectors and consist of various materials and components. Moreover, plasma heating systems and diagnostics add up to the packed surrounding in the reactor hall. This plays a significant role in neutron measurements mainly due to the strong scattering of neutrons. Further, neutron interactions depend on material composition and thickness. To capture these effects, a toy train carrying a radioactive source (^{238}Pu/B) was continuously run over two radial positions on the equatorial plane inside the tokamak vessel (figure 1 (a)). The neutron spectrum of the source has a Maxwellian distribution peaked at 2.8 MeV which is nearly the energy of D-D neutrons produced at AUG. The emitted neutrons are collected by thermal neutron detectors positioned outside the machine. AUG is equipped with ^{3}He and BF_3 detectors, and several fission chambers placed inside a detector box which can be translated and rotated in space (figure 1 (b)). The high energy

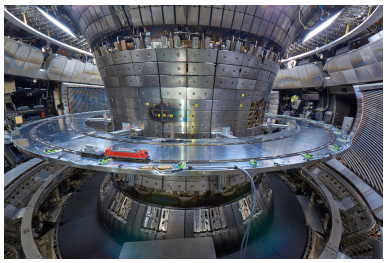

(a) Inside AUG vessel

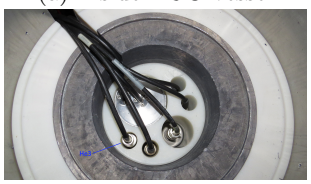

(b) END top view

Figure 1: Radioactive source (^{238}Pu/B) on top of a toy train running on two radial positions inside the tokamak vessel (a) and the ASDEX Upgrade epithermal neutron diagnostics (END) (b).

neutrons are slowed down to thermal energies ($\approx$ 0.025 eV) by a double layer of polyethylene moderator, while the layer of lead in between blocks the gamma rays that usually accompany radioactive sources and tend to distort the neutron signal. The emitted neutrons pass through the vessel components and the support structure. Hence, detailed AUG geometry and precise density values of each material are necessary for reliable transport simulations. This work focuses on the absolute calibration of the ^{3}He detector and compares the experimental results to the simulations performed with the Serpent code.

Helium-3 interacts strongly with thermal and epithermal neutrons due to its high cross-section for this energy range and its sensitivity to gamma rays is negligible. The total macroscopic cross-section, $\Sigma = N\sigma$, where N is the atomic density of the target and σ is the microscopic cross-section, is shown in figure 2. This type of detector works

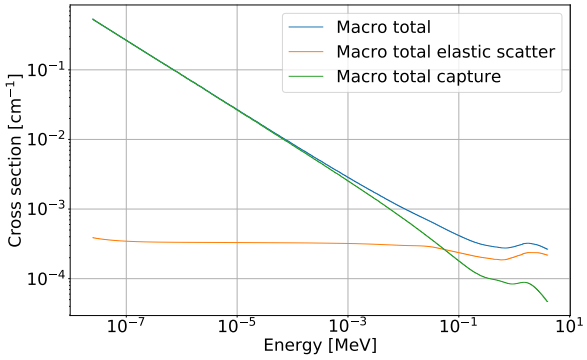

Figure 2: ^{3}He cross-sections generated with the Serpent code.

through (n,p) nuclear reactions:

$$^3\text{He} + \text{n (thermal)} \rightarrow {}^1\text{H} + {}^3\text{H} + \text{Q (764 keV)}$$

resulting in a prompt proton and tritium and releasing kinetic energy of 764 keV shared between the daughter products. ^{3}He is a proportional gas detector. The proton ionizes the gas atoms, creating charges which further ionize the medium in an avalanche process and are collected as electric pulses [8].

3. Simulation of the n-rate in AUG with the Serpent code

Neutron transport models rely on statistical methods that track the particle paths and calculate probabilities for numerous events. Monte Carlo transport codes are one example of such approach that simulates histories of particles traversing modelled geometries.

The most convenient way to incorporate a detailed ASDEX Upgrade model inside Serpent is using stereolithography (STL) files. For that purpose the whole machine was decomposed into smaller parts using the CAD software CATIA [9] and converted to STLs. The AUG assembly is organized in 16 sectors that can be further arranged in five main segments - vessel, magnetic field coils, turn-over structure, inner tiles and divertor (fig. 3). The poloidal field coils and the support structure of the vessel are also included in the simulations. The detector chamber was

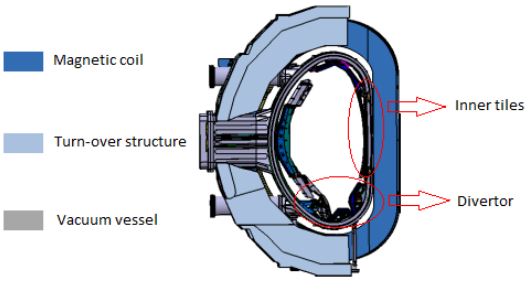

Figure 3: ASDEX Upgrade sector the from CATIA software.

divided into moderator, lead blocks and ^{3}He tube.

The main reason for such a fine geometry splitting is the fragile STL mesh. Crucial for STL objects is to be watertight. Conversion to STL of sophisticated or ambiguous geometries may introduce mesh failures in the forms of holes, wrong facets or coinciding points that break the watertightness of the model. In Monte Carlo methods faulty STL files can lead to poor simulation performance, misleading results and can even terminate the calculation. The watertightness of the implemented parts could be checked within Serpent thanks to a special test-option included in the code. Recommended consistency levels are above 90%. Nonetheless, the files should be fixed in a CAD software or with specified STL repairing tools. In this task, the faulty STLs were fixed using the repairing program NetFabb [10].

Every STL object is assigned a material using material cards. Material definitions follow two main parameters - density and mass or atomic fractions of the constituent nuclides. Each nuclide is given a temperature and linked to a cross-section library [11]. Incorporated libraries provide data for thermal and higher energy cross-sections of numerous nuclides.

Most of the AUG materials like stainless steel, copper and graphite have well documented properties and can be easily found at open web sources. This does not hold, however, for the polyethylene density. Conveniently, Serpent provides a list of material compositions taken from the "Compendium of Material Composition Data for Radiation Transport Modeling" [12]. For the calculation of the gas density we assume a pure ^{3}He and we take the nominal pressure from the data sheet of the detector.

To calculate reaction rates (RR) Serpent solves an integral of the form:

$$RR = \frac{1}{V}\int_V \int_E \int_{\hat{\Omega}} \int_t f(r,\hat{\Omega},E,t)\Phi(r,\hat{\Omega},E,t)d^3rdEd\Omega dt \quad (1)$$

where V is the volume of the specified region, f is the response function, Φ is the particle flux and 1/V is a normalization factor, which by default is set to unity. The response function is a microscopic or macroscopic cross-section that yields the corresponding RR.

In this work we compute the flux passing through the ^{3}He counter and the corresponding (n,p) reaction rate. The detector tube has an active length with radius R = 1 cm and a height H = 31 cm. The helium density specified by the manufacturer is 0.5×10^{-3} g/cm^3. All cross-section data in this work are taken from the incorporated Serpent libraries.

4. Comparison between measurement and Serpent simulation

In this section we present the results from three calibration measurements - two inside the vacuum vessel and one outside. Measurements with the toy train were carried out for a total of one weekend (one day one radial position). The recorded data acquisition exceeds 130k seconds. The smoothed neutron rate from the outer railway track for 5000 s and the corresponding average NR are shown in figure 4. The average period of a full toroidal turn is ≈ 280 s. The displayed background noise is roughly 0.04 n/s and it represents the measured NR inside the AUG hall in the absence of the calibration source.

Serpent calculations were performed without medium using a point source of 2.7 MeV on an outer railway track position with a direct view to the detector box. The cross-section libraries assigned to the materials are valid for thermal energies.

To check how the vessel components affect the NR, AUG sectors, copper coils and support structure (SS) were gradually added to the geometry (Table 1). Calculations

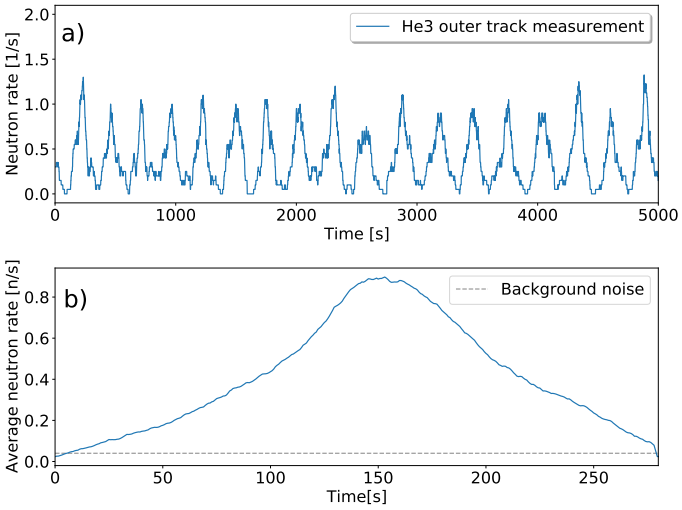

Figure 4: ^{3}He neutron rate signal, measured with the toy train on the outer railway track (a) and the calculated average neutron rate peak for that signal (b).

only with detector box and a point source show an NR of roughly 145 n/s which decreases by 2 when sector 9 and 11 are included. This leads to a discrepancy factor of about 70 between the experiment and the simulation. However, adding the whole geometry significantly enhances the NR, possibly due to strong scattering from the additional components, and eventually results in a discrepancy factor of roughly 130 between the experimental NR and simulation.

To understand the huge disagreement we completed

Sectors	Flux [n·cm]/s	(n,p) [n/s]
No sectors	923.614	144.516
11	419.936	68.441
9 and 11	533.256	67.96
all	623.097	108.0235
all with coils	582.450	114.784
all with coils and support structure	652.444	134.9207

Table 1: Comparison of the neutron rate predicted by Serpent adding gradually different AUG components.

a measurement outside the tokamak with a clear view to the detector box choosing three positions (30, 100 and 190 cm) away from it.

We executed two simulations - one only with detector box and one with detector box and the AUG machine (figure 5 (a, b)). The comparison shows a systematic factor of average 5.5 between Serpent and the experimental NR which increases to roughly 6 if the reactor is added. This shows that the neutron scattering from the vessel for this set-up is small. Its importance becomes significant when the measurements are taken on the opposite side of the box (figure 5 (c)). Experimental results led to roughly 80 n/s or 11 times less if we simulate only the detector chamber. The simulated NR is 30% higher when the vessel is included. From this we presume that the dis-

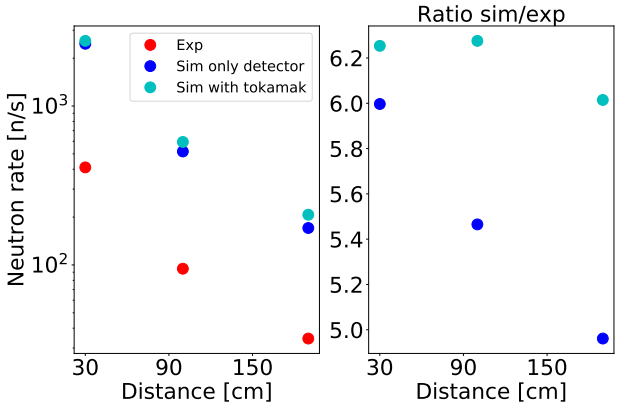

(a) Total neutron rate

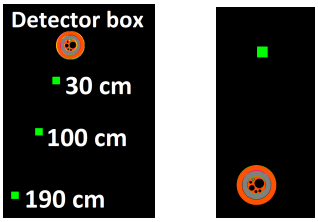

(b) Source positions outside of the reactor, opposite the vessel (left) and on the side of the vessel (right)

Figure 5: Comparison between the experimental NR and the one predicted by Serpent (a) for three different positions from the detector box outside of the tokamak vessel ((b), left).

crepancy is sensitive to the moderator thickness (radial source position) and the simulation geometry. Insufficient or huge thicknesses are not able to slow down the neutrons or absorb most of them, respectively. The counter is exposed to different moderator thicknesses due to its non-symmetric position inside the chamber which impacts the incoming neutron flux. More detailed investigations

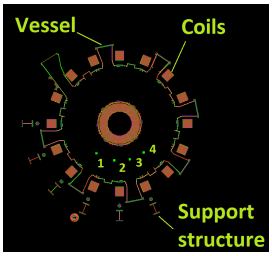

(a) Four source positions inside the AUG machine

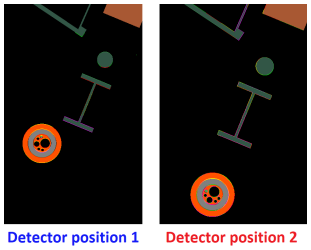

(b) Detector configurations

Figure 6: Geometry set-up for the four source position measurements inside the vessel and two detector configurations.

outside the vessel are necessary to provide a clearer understanding of the factor in that regard. Such are, however, difficult to complete due to the limited free space around the chamber. The mobility of the detector could be used to further examine the detector response. In the third calibration measurement we chose four source positions inside the tokamak with known distance and height relative to the vessel components ((figure 6 (a)). For two of them we changed the detector configuration as shown in figure 6 (b)). The results for detector position 1 are presented in figure 7. Here, the factors for positions 2, 3 and 4 fluctu-

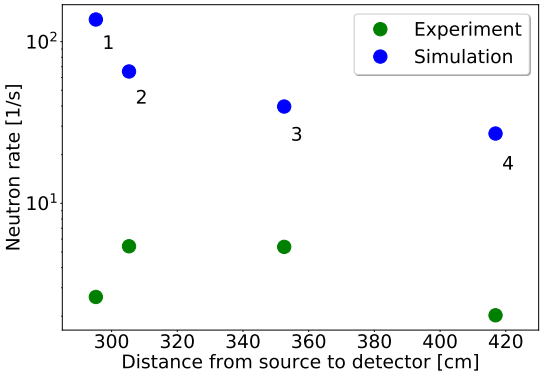

Figure 7: Comparison between the experimental NR and the simulation for four different source positions inside the tokamak.

ate roughly between 7 and 14 which fits reasonably well the error from the measurements outside the reactor. Position 1 is a strong exception to this pattern. The reason for this is likely to be missing components around the detector chamber which may decrease the incoming neutron flux. In a close proximity to the box is the interferometer diagnostics which is enclosed between two carbon epoxy walls. The carbon as a light element is expected to slow down the neutrons around this sector of the vessel. The ICRF limiters which are also made from carbon and currently not included in the simulation are another potential candidate. The components are yet to be included in the geometry.

The same measurement was repeated for detector configuration 2 for two of the source positions (figure 8). The NR drop due to the support structure column on the line of sight of the detector is visible in both experiment and simulation. The discrepancy remains within the already observed range (factor 14 for position 2 and factor 18 for position 4). This is clearly observed also in the detailed

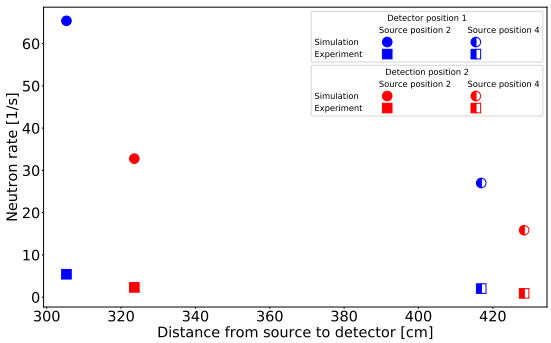

Figure 8: Comparison between the experiment and the simulation for two source positions inside the tokamak with two detector configurations.

comparison for one toroidal train turn inside the tokamak (figure 9). We define $\theta = 0$ to be the closest (and with the

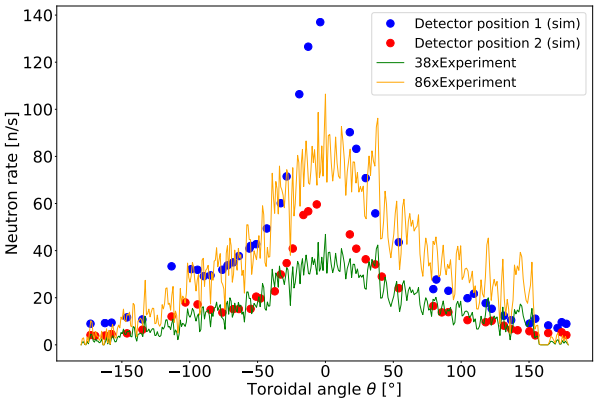

Figure 9: The average experimental NR (solid line) vs the NR computed with Serpent (points) for one toroidal train turn and two detector configurations.

least material in the simulation) position of the train to the detector chamber. The two fitting factors match the minimum mean squared deviation. Both fits fail to describe well the NR in angles $\theta = \pm 21$ degrees. In this range the source passes only through the thin stainless steel layer ($\approx$ 5 cm) of the vessel port. The train is in the line of sight of that area also for angles θ = -118 to -95 degrees, resulting in the observed NR bumps. Nonetheless, the fit appears to describe aptly the rest of the simulated data. However, factor 86 is too high and not in agreement with the previous discrepancy investigations. Hence, we presume that the train measurements correspond to the second position (figure 8) of the detector. The factor around the peak is expected to drop when the interferometer wall is integrated into the geometry. Effect on the edge data is also not excluded. The ICRF limiters may also contribute.

5. Summary and conclusions

Three sets of calibration measurements of the ^{3}He thermal neutron detector were performed at ASDEX Upgrade and simulated using the Monte Carlo transport code Serpent. A detailed geometry of AUG was decomposed, converted to STL files and implemented in the code. Comparisons between the experimental NR and the simulation outside the vacuum vessel resulted in a varying factor (between 5 and 15) with respect to the radial source position. The paper proves that the difference likely depends on the polytheylene thickness.

The impact of the geometry on the detector response was tested for one source position by gradually adding up vessel components. The simulated NR was found to exceed the toy train measurement by a factor of 130 in the position of least material in the line of sight to the detector box. Suggested explanation for the huge difference is the missing interferometer close to the detector chamber. The carbon epoxy wall of the diagnostics is expected to decrease the neutron rate due to the strong moderating property of the material.

Calibration measurement with four fixed source positions inside the tokamak and two detector configurations confirms that the discrepancy factor is sensitive to the moderator thickness and scattering from the reactor components. The varying factor for both detector locations (7 vs 18) is consistent with the outside vessel calculations. Probing experimentally sufficient source positions around the detector chamber is needed for further understanding of the factor. The difficulty to carry out such a study comes from the limited free space around the detector.

For measurements inside the torus the discrepancy factor is higher, $\approx$ 38, and even higher close to the position of the maximum NR. In this range inside the simulation the neutrons pass through a very clear view to the box with almost no material on the way. The factor is expected to drop when the interferometer diagnostics is included in the geometry. ICRF limiters are also expected to affect the simulated neutron rate.

Acknowledgements

This work has been carried out within the framework of the EUROfusion Consortium and has received funding from the Euratom research and training program 2014–2018 and 2019–2020 under grant agreement No. 633053. The views and opinions expressed herein do not necessarily reflect those of the European Commission.

References

[1] J. Eriksson, C. Hellesen, F. Binda, M. Cecconello, S. Conroy, G. Ericsson, L. Giacomelli, G. Gorini, A. Hjalmarsson, V. G. Kiptily, M. Mantsinen, M. Nocente, A. Sahlberg, M. Salewski, S. Sharapov, M. T. and, Measuring fast ions in fusion plasmas with neutron diagnostics at JET, Plasma Physics and Controlled Fusion 61 (1) (2018) 014027.

[2] G. Tardini, C. Höhbauer, R. Fischer, R. Neu, Simulation of the neutron rate in ASDEX upgrade h-mode discharges, Nuclear Fusion 53 (6) (2013) 063027.

[3] R. Hawryluk, An empirical approach to tokamak transport (12 1981).

[4] H. Hendel, R. Palladino, C. Barnes, M. Diesso, J. Felt, D. Jassby, L. C. Johnson, L. Ku, Q. Liu, R. Motley, H. B. Murphy, J. Murphy, E. Nieschmidt, J. A. Roberts, T. Saito, J. Strachan, R. J. Waszazak, K. Young, In situ calibration of TFTR neutron detectors, Review of Scientific Instruments 61 (1990) 1900–1914.

[5] P. Batistoni, S. Popovichev, S. Conroy, I. Lengar, A. Čufar, M. Abhangi, L. Snoj, L. Horton, Calibration of neutron detectors on the joint european torus, Review of Scientific Instruments 88 (2017) 103505.

[6] T. Nishitani, K. Ogawa, M. Isobe, H. Kawase, N. Pu, Y. Kashchuk, V. Krasilnikov, J. Jo, M. Cheon, T. Tanaka, S. Yoshihashi, S. Li, M. Osakabe, Calibration experiment and the neutronics analyses on the LHD neutron flux monitors for the deuterium plasma experiment, Fusion Engineering and Design 136 (2018) 210–214.

[7] J. Leppänen, M. Pusa, T. Viitanen, V. Valtavirta, T. Kaltiaisenaho, The serpent monte carlo code: Status, development and applications in 2013, Annals of Nuclear Energy 82 (2015) 142 – 150.
[8] G. F. Knoll, Radiation detection and measurement, Wiley.
[9] www.technia.de/software/catia/, Catia v5.
[10] www.autodesk.de/products/netfabb/, Netfabb.
[11] J. Leppännen, Serpent - a Continuous-energy Monte Carlo Reactor Physics Burnup Calculation Code, 2015.
[12] R. Mcconn, C. Gesh, R. Pagh, R. Rucker, R. Williams, Compendium of material composition data for radiation transport modeling (01 2011).